Centrifuge Investigations of Reverse Fault Interaction with Jack-up Rig Spudcan Foundations

K.J. Oakes*, M.J. Brown and J.A. Knappett
School of Science and Engineering
UNIVERSITY OF DUNDEE

I. Anastasopoulos
Institute for Geotechnical Engineering (IGT)
ETH ZÜRICH

** corresponding author: koakes@dundee.ac.uk*

ABSTRACT
This paper introduces the methodology for a series of centrifuge model tests which investigated the interaction between geological faults, in sand and a jack-up rig with spudcan foundations. Understanding the fault rupture–soil–foundation–structure interaction (FR-SFSI) is critical when attempting to develop platform design and risk mitigation strategies. The findings may be used alongside other hazard risk mitigation strategies deployed during site investigations and assessments of rig operations. Results show how a reverse fault propagates though the soil and directly intercepts the spudcan foundations. The jack-up causes fault diversion and bifurcation yet still suffers from significant rotations at the hull and large axial forces in the legs. This research forms part of a wider study which includes finite-element analyses (FEA) of the jack-up-fault interaction. The centrifuge results will be used to validate and further calibrate the numerical analyses.

KEYWORDS*: earthquake engineering, marine engineering, geological faults, jack-up spudcan foundations, soil-structure interaction, centrifuge testing, sand.*

INTRODUCTION

A jack-up is a mobile platform used globally within the oil and gas industry for exploration and production. They are also used in the deployment of offshore wind farms. The interaction between earthquake faults and jack-up rigs has received little attention in the scientific literature and yet these multi-million-dollar structures are continually deployed in seismically active regions throughout the world. During an earthquake, transient shaking takes place and propagates seismic waves long distances throughout the seabed. This alongside the permanent ground displacements that take place can have a significant effect upon structures situated on the seabed [2]. This latter problem, known as 'fault rupture-soil-foundation-structure interaction' (FR-SFSI), refers to the interaction of a fault which propagates towards and ruptures at the ground surface, whilst deforming the soil and interacting with foundation-structure systems. In the free-field, where no structure is present, it is well-documented that the propagation path and the surface scarp magnitude are dependent upon three factors: the overlying soil (stiffness and strength), the magnitude of fault offset at bedrock and the type of fault— dip-slip or strike-slip [9 & 3]. When interacting with a structure, the extent of soil deformation can vary and in some cases the fault can be diverted when the structure is heavily loaded and the bearing stresses are large enough, as is the case for a continuous and rigid foundation system [1 & 3]. On the other hand, lighter structures can slip and rotate on their foundations, or the foundations themselves may rupture as the fault ruptures through the soil [1 & 5]. After a series of earthquakes in Taiwan and Turkey in 1999, [3] documented the significant effects a dip-slip fault can have upon a structure — severe damage and even structural collapse was observed as a result of fault displacements ranging from 2 m to 8 m.

At the University of Dundee extensive research has been carried out investigating FR-SFSI with a variety of structures and soil material. Experimental faulting research has taken advantage of the well-controlled laboratory environment and through the use of a geotechnical centrifuge has investigated interaction between faults and structures including pipelines [14], caisson foundations [13] and strong raft foundations [10]. [1] investigated the interaction of shallow, rigid foundations with reverse faults and found the response of the foundation very sensitive to the proximity of the fault. According to [1], the two main indicators of foundation distress are excess foundation rotations (as a result of differential settlement), causing distress to the above structure [8] and, the generation of a gap beneath the foundation resulting in bearing pressure redistribution

between the foundation and the soil, an effect which [4] suggested may induce extreme bending moments in the foundation. [14] determined that the rigid body of a buried caisson acted as a kinematic constraint and forced the rupture to divert or bifurcate around the structure, this mechanism also occurred with raft foundations, shallow rigid foundations and pipelines [11; 1 &15]. [4] on the other hand suggested such mechanisms do not always occur with shallow foundations and that a fault can emerge beneath the foundation, causing a gap to form.

A jack-up rig being subjected to tectonic displacements, coupled with the risk of operating in an offshore environment, could prove catastrophic for the platform and for personnel on-board where tight tolerances on rig rotations are normally adopted. There is little information in codes and guidelines on faulting in an offshore environment and how best to mitigate the hazard. This paper forms part of a wider project which utilises experimental and numerical procedures to investigate the FR-SFSI of normal and reverse faults with jack-up rigs and can be used as a means of risk mitigation and to assure platform integrity. Using the University of Dundee 3 m radius geotechnical beam centrifuge and a specially developed in-flight earthquake faulting box this paper considers the propagation and rupture of a reverse fault through dense sand and investigates the interaction with a model jack-up rig. A basic schematic of the problem is shown in Figure 1 whereby a fault propagated and ruptured at the soil surface between the legs of the rig. A jack-up rig with shallow spudcan foundations was embedded into the ground surface, after which the fault propagated from the bedrock through the sand layer. Influenced by the size of the fault throw, *h*, the overlying material and the fault type, the fault may propagate and rupture at the ground surface, potentially interacting with the foundations of the structure. The fault dip angle at bedrock was controlled by the split box but may change as the fault propagates through the soil and approaches the surface. Free-field tests conducted in the absence of a structure determined the free-field fault rupture location. The distance from this location to the left edge of the bow spudcan is represented by the spacing, *S* (see Figure 1). The location of the structure can be normalised by the foundation breadth, *S*/*B*. Depending on the structural position relative to the fault surface outcrop, it may undergo displacements and rotations at the footings and hull.

The constitutive behaviour of soil is non-linear and dependent upon the stress levels in the soil medium. The centrifuge model and its prototype will be geometrically similar, with scaled down linear dimensions and structural stiffness, so as to capture the behaviour of the prototype and the in-situ effective stresses. To achieve this, the unit weight of the soil was increased by accelerating the model in a centrifuge. As the stress in the soil was increased, the propagation of the fault may vary when compared to reduced scale 1-g tests. It is practically impossible to directly replicate all behavioural aspects of a full-scale prototype. This is where the benefits of the centrifuge become apparent, as many of the difficulties in scaling can be avoided if the stresses at corresponding points in the model and prototype are the same. As long as these corresponding points are geometrically equivalent, the stresses will be the same. Using generalised centrifuge scaling laws, the principle of "modelling of models" was applied. As in [18 & 19], the prototype (rig) was scaled down (using factor μ) creating a virtual 1-g model, which was subsequently scaled down again (by factor η) to create the physical centrifuge model. The scaling factors were multiplied, resulting in a much larger effective scaling factor, λ, creating the relationship $\lambda = \mu\eta$, as shown in Figure 2. For these tests $\lambda = 300$ and hence the centrifuge model has been scaled down 300 times. The use of generalised scaling and such a large value of λ was necessary given the large size of jack-up rigs and the container size in the centrifuge.

METHODOLOGY

The centrifuge strong box, previously used by [1; 11; 14 & 15], had internal dimensions measuring 800 mm x 500 mm x 500 mm. Two sides of the model were visible through transparent Perspex plates. A split box system was inserted into the bottom of the strong box, leaving an area above to develop the soil model with internal dimensions measuring 655 mm x 500 mm x 250 mm (Figure 3). The base of the split box consisted of a moveable triangular base block, stationary aluminium (aluminium alloy 6082T6) blocks and a singular composite block of concrete and aluminium (Figure 3). The moveable block was supported and repositioned in-flight using two hydraulic jacks with a 300kN load capacity to simulate the fault loading. The left boundary of the model was retained by a vertical plate on the side of the split box which was attached to the moveable base block, thus ensuring the left side and base block moved as one during the faulting event. When conducting reverse faults, whereby this moveable section was shifted upwards and to the right, aluminium spacer blocks were added to ensure the block did not drop downwards during the initial stages of the test. During normal

fault tests these spacer blocks (Figure 3) were removed allowing the block to move downwards and left during fault displacement. Whilst the centrifuge was spinning-up to the determined g-level the moveable blocks were retained in place by the hydraulic jacks. The right boundary of the model was in contact and retained by the opposite side of the strong box. Sandpaper sheets were attached to the vertical and base surfaces of the split box so as to recreate a rough rock-soil interface. Where the moveable blocks slid against the stationary blocks of the faulting apparatus, PTFE plates with a coefficient of friction of 0.1 were bolted to the interfaces allowing reduced frictional forces and smooth faulting displacements. PTFE plates were also placed along the surface of the reverse fault spacer blocks. The hydraulic jacks and the aluminium and composite blocks were inclined about the horizontal axis so as to create a fault (in the bedrock analogue) with a dip angle of $\alpha = 60°$. The hydraulic jacks were attached to a hydraulic pump, pressure gauge (capacity 25MPa) and a non-return valve, connected through the hydraulic slip ring, and controlled from outside of the centrifuge.

HST95 Congleton silica sand was used throughout the project which is a fine, uniformly graded sand, characterised by a sand unit weight = 16.75 kN/m^3, critical state friction angle $\phi = 32°$, maximum dry density = 17.58 kN/m^3, minimum dry density = 14.59 kN/m^3 and $D_{50} = 0.14$ [13]. The sand was sieved and prepared using a sweeping pluviator to create 20–30 mm thick dense layers. To aid in monitoring the deformation through the Perspex window, each layer had a line of dyed sand (~2 mm thickness) added on top and adjacent to the Perspex window. Repeating this process, pluviation continued to create a soil depth of 200 mm, or 60 m at prototype scale with a relative density $D_r \approx 80\%$. Density pots were used as a means of checking the homogeneity of the model and the model was weighed to verify this. Dyed sand was applied to the surface of the top soil layer to further aid in geomorphological analysis of the fault expression in plan.

The rig dimensions were based upon scaled (200g) jack-up centrifuge tests conducted by [6] with key components alongside sign conventions and loading directions shown in Table 1 and Figure 4. Numerical FEA work verified that the model tests were not influenced by boundary conditions. Model and prototype jack-ups are typically built from different materials (aluminium and steel respectively) and as a result have a different Young's modulus. *EA* and *EI* must be scaled correctly rather than the individual properties of *E*, *A* and *I*. The correct scaling of the flexural stiffness was prioritised. The gravitational field of the centrifuge increased with distance away from the rotational centre. Consequently, the acceleration varied along the model height. Priority was placed upon correctly modelling the foundation-soil interaction and the soil stress field there, thus the acceleration was set to 75 g at the soil surface. [6] stated that the response of the model jack-up was due to the footing reactions at an elevated g level and thus applied the same acceleration at the soil surface when converting results to prototype scale using the scaling laws. Given the height of the model rig, the scaling factor, *N* varied between the hull ($N = 60$) and the footings ($N = 75$), however strain gauges on the legs measured the axial force, ensuring that the loads applied to the spudcans were accurately known.

During the operation of a full-scale rig, the spudcans can be embedded into the soil due to a preloading phase whereby seawater is pumped into the rig as a ballast, increasing the weight of the rig to say twice the operating weight to allow safe in-service operation. In this research a weight plate (model = 0.57 kg, prototype = 15,560 t) was added on top of the hull to recreate this preload weight. To allow for this preloading process, the centrifuge testing was conducted in two phases. The initial phase included a spin up to 75 g with the preload weight resting on top of the hull causing the rig to embed. The centrifuge was then stopped to allow the removal of the preload weight plate. Once removed, the second phase was undertaken whereby the target g level was reached as the rig sat freely under its own self-weight and the fault was applied.

The rig was instrumented to allow detailed measurements to take place during both phases of the testing and logged through a custom built data acquisition system. Instruments included:

- strain gauges (Micro-measurements, L2A-13-250LW, 120Ω resistance, 5V supply) logging leg bending moments, axial forces and shear forces (L2A-13-062LV),
- an accelerometer (Analog Devices EVAL-ADXL377Z, 3-axis, range of ±200 g, bandwidth range of 0.5–1300 Hz for the x-axis and y-axis and 0.5–1000 Hz for the z-axis, accelerometer measuring 3 x 3 x 1.45 mm, 2.5V supply) allowing inclinations at the hull reference point (HRP) to be recorded as in [16] and,

- an LVDT (RDP Spring Return, LDC1000A, ±25 mm, 5V supply) mounted onto a section of the moveable split box to measure the fault throw, *h*.

RESULTS AND DISCUSSION

This paper considers results for a structural-reverse fault test. The response of the rig is discussed in terms of the rotations at the HRP (θ_x, θ_y and θ_z or rig roll, tilt and twist respectively) and the axial force on the footings, measured respectively by the accelerometer fixed to the hull and strain gauges on the legs. A reverse fault was applied with a throw of h = 33.4 mm (10.03 m prototype), causing the rig to tilt by pushing the rig upwards (at the bow leg) and towards the stern (Figure 5). The horizontal inked layers of sand show the expression of the fault as it propagated upwards towards the soil surface where it was seen to outcrop as shown in Figure 5. Once faulting had begun, 0.82 m of fault throw had occurred before the fault ruptured at the surface of the soil and was measured within the instrumental data (accelerometer and strain gauges). This occurrence is shown in Figures 6 and 7 whereby the change in compressive axial forces and the inducement of hull rotations signified the start of the fault-soil-structure interaction. This was consistent with significant volume change being required in the soil before localisation and complete propagation of the fault to the soil surface.

The reverse fault propagated through the soil and ruptured at the surface, in between the foundations of a jack-up rig at S = -36.67mm (-11 m prototype) from the fault. The normalised structural location was S/B = -3.67. The port and starboard footings sat on the static footwall whilst the bow spudcan was situated on the hanging wall of the fault (Fl) (Figure 5). Consequently, the bow spudcan was displaced upwards and to the stern. Figure 5 shows the evolution of the faulting process with reference to the free-field (no structure present) test. Shortly after fault activation and as a result of the high relative density of the soil, a steep shear deformation (F1) propagated through the sand and ruptured at the surface, approximately following that of the free-field propagation path (FF). With further faulting, a second failure surface, F2, began to propagate through the soil but did not reach the surface, instead only shearing up to about one-third of the soil model. Continued bedrock offset induced the development of a failure wedge at the surface of the soil causing the fault to bifurcate along plane F3. The evolution of multiple failure planes is consistent with the development of shear deformations observed by [1; 12 & 14].

After propagating through about half of the soil, Figure 5 shows that the dip of the shear bands (F1 & F3) reduced, causing a change in fault direction, a mechanism observed by [1; 10 & 17]. This fault diversion was influenced by the presence of the structure, a mechanism partly controlled by the bearing pressure of the foundation and the proximity of the structure. This observation coincides with other studies [11; 12 & 15] concluding that foundations can force the fault rupture to deviate if they are continuous, rigid and or have significant surcharge loading. [1] found a bearing pressure measuring q = 37 kPa significantly diverted the fault. At 75g, or operating g-level, the jack-up at induced a total vertical force of 136 MN, causing a maximum bearing pressure of q = 636 kPa per footing on the soil. Thus it is expected that fault diversion is likely.

The total weight of the rig was not initially expected to distribute evenly throughout the structure due to difficulties in placing the structure entirely flat on the soil surface. Figure 6 shows the maximum axial force on each footing due to the self-weight of the rig was ~50 MN port and starboard and ~36 MN bow, inducing a maximum footing bearing pressure of 636 kPa. These forces were consistent with the weight of the prototype rig (136 MN). Both Figures 6 & 7 show that overall the jack-up rig experienced significant upward movement and unloading within the bow leg and spudcan, tilting the rig, causing the port and starboard legs and spudcans to counteract by compressing and embedding further into the soil. When the fault on plane F1 initially ruptured the soil surface at h = 0.82 m and continued for 2 m, the bow leg saw an increase in compressive force by 2.75 MN, whilst the starboard leg reduced in compressive axial force by 2.74 MN, thus balancing the change in axial force (Figure 7). The port leg on the other hand saw little change, this may be due to instrumentation installed on the rig causing the self-weight force of the structure not to be distributed evenly throughout the rig. As fault displacement continued along F1 to h = 6.89 m, the axial forces became reversed and the bow leg experienced a significant reduction in compressive axial force of 17.55 MN, whilst the opposing port and starboard legs counteracted this with increases of 7.49 MN and 9.42 MN respectively, hence approximately balancing the actions of the bow leg with a combined change of 16.90 MN. As a result the rig tilted towards the stern by 3.7° (Figure 7), an element of bending moment was induced on all legs and the legs became inclined. Each jack-up has its own rotational limits and whilst there appears to be no code or standard for it values of 0.2° (for extreme operational conditions) and 1° (during leg lifts) have been detailed in designer manuals. A rig tilt of 3.7° is thus considered very extreme and well beyond the design limits of the structure.

The effect of changes in axial force with increasing fault throw did not continue throughout the test and stopped at approximately 6.89 m, whereby at which time F1 became inactive and fault deformation propagated only along F3. This mechanism was consistent with [14]. Deformation along shear plane F3 continued from h = 6.89 m to h = 10.03 m and appeared to have only had a very small influence upon the structural response. The port leg sees an increase of 0.87 MN in axial compression whilst the starboard decreases by 0.4 MN (Figure 7). Since there is no rolling of the rig (no change in θ_x, Figure 7) and these force changes are soon reversed, it is believed the rig has redistributed forces throughout the structure, a phenomenon observed by [6]. As [7] discusses, this highlights the importance of analysing the rig as a complete system as the spudcans are linked by the superstructure and therefore the yielding of one footing does not necessarily imply failure for the whole rig. No change in axial compressive force was observed in the bow leg by F3. The port and starboard legs fluctuated minimally yet ensured the rig was balanced throughout the remainder of the test. When compared to F1, the insignificance upon structural behavior of shear band F3 was also reflected in the tilting action of the jack-up. Figure 7 shows significant tilting from h = 0.82 m to h = 7 m inducing hull rotation of 3.7° as F1 deformed the soil. Beyond h = 6.89 m there was no further change in hull rotation. This finding also indicates how the effect of fault F1 diminished within the latter stages of faulting, a process thought to be influenced by the structural presence and its capacity to diffuse the shear band.

CONCLUSIONS

This paper has introduced a method to determine the interaction between typical jack-up rig and normal and reverse faults at stress levels experienced by a prototype rig. The correct scaling laws were prioritised when designing the rig, as was the avoidance of parasitic boundary conditions. Preliminary findings of a reverse fault test show that:

- As found in previous research on the topic, foundations with a large surcharge weight can divert the fault, cause it to bifurcate and diffuse the shear band created by the fault. The jack-up rig acted as a kinematic constraint forcing the fault to bifurcate and divert around the structure. This potentially limits the faulting effects upon the structure.
- The influence of the active fault F1 diminishes with time by the presence of the structure acting to diffuse the shear band.
- The fault causes significant interaction with the structure, inducing large changes in axial force within the legs and causing the rig to tilt significantly at the hull level, well beyond operational design limits.
- Load redistribution amongst the footings takes place towards the latter stages of the test, highlighting the importance of considering the whole superstructure when conducting analyses.

Work is ongoing to analyse the data further and determine the structural or operational significance of the results shown here for jack-up operation. These findings are being used to validate the effectiveness of numerical models developed to address the problem, results of which will be published in the future.

ACKNOWLEDGEMENTS

The work contained in this paper was conducted during PhD study undertaken as part of the Natural Environment Research Council (NERC) Centre for Doctoral Training (CDT) in Oil & Gas [grant number NEM00578X/1] and was match-funded by the University of Dundee.

REFERENCES

[1] Ahmed W, Bransby MF Interaction of Shallow Foundations with Reverse Faults, Journal of Geotechnical and Geoenvironmental Engineering. 2009:135(7):914–924.

[2] Anastasopoulos I, Gazetas G, Bransby MF, Davies MCR, El Nahas A Fault Rupture Propagation through Sand: Finite Element Analysis and Validation through Centrifuge Experiments, Journal of Geotechnical and Geoenvironmental Engineering, ASCE. 2007:133(8):943–958.

[3] Anastasopoulos I, Callerio A, Bransby MF, Davies MCR, El Nahas A, Faccioli E, Gazetas G, Masella A, Paolucci R, Pecker A, Rossignol E Numerical analyses of fault–foundation interaction, Bulletin of Earthquake Engineering. 2008:6(4):645–675.

[4] Anastasopoulos I, Gazetas G, Bransby MF, Davies MCR, El Nahas A Normal fault rupture interaction with strip foundations, Journal of Geotechnical & Geoenvironmental Engineering, ASCE. 2009:135(3):359–370.

[5] Berill JB Two-dimensional analysis of the effect of fault rupture on buildings with shallow foundations, Soil Dynamics and Earthquake Engineering: 1983:2(3):156–160.

[6] Bienen B, Cassidy M, Gaudin C Physical modelling of the push-over capacity of a jack-up structure on sand in a geotechnical centrifuge, Canadian Geotechnical Journal. 2009:46:190–207.

[7] Bienen, B. Three-dimensional physical and numerical modelling of jack-up structures on sand. UWA: 2007:PhD Thesis.

[8] Bird JF, Bommer JJ, Crowley H, Pinho R Modelling liquefaction-induced building damage in earthquake loss estimation, Soil Dynamics & Earthquake Engineering. 2006:26(1):15–30.

[9] Bray JD, Seed RB, Cluff LS, Seed HB Earthquake Fault Rupture Propagation through Soil. Journal of Geotechnical Engineering. 1994:120(3):543–561.

[10] Cole DA Jr, Lade PV Influence zones in alluvium over dip-slip faults. Journal of Geotechnical Engineering. 1984:110(5):599–615.

[11] El Nahas A, Bransby MF & Davies MCR. Zhang & Wang, editors. Physical Modelling in Geotechnics. London. 2006.

[12] Gazetas G, Zarzouras O, Drosos V, Anastasopoulos I Bridge–Pier Caisson foundations subjected to normal and thrust faulting: physical experiments versus numerical analysis. Meccanica. 2014:50(2):341–354.

[13] Lauder K, Brown MJ, Bransby MF, Boyes S The influence of incorporating a forecutter on the performance of offshore pipeline ploughs, Applied Ocean Research. 2013:(39):121–130.

[14] Loli M, Bransby MF, Anastasopoulos I, Gazetas G Interaction of Caisson Foundations with a Seismically Rupturing Normal Fault: Centrifuge Testing versus Numerical Simulation, Geotechnique. 2012:62(1):29–43.

[15] Nagaoka S The Interaction of Earthquake Faults with Foundations and Pipelines. PhD Thesis, University of Dundee. 2012.

[16] Robinson S, Brown MJ, Matsui H, Brennan A, Augarde C, Coombs W, Cortis M. Centrifuge testing to verify scaling of offshore pipeline ploughs, International journal of physical modelling in geotechnics. 2018

[17] Roth WH, Scott RF, Austin I Centrifuge modelling of fault propagation through alluvial soils, Geophysical Research Letters. 1981:8(6): 561–564.

[18] Schofield AN Cambridge geotechnical centrifuge operations, Géotechnique. 1980:30(3):227–268.

[19] Tobita T, Escoffier S, Chazelas J-L, Iai S Generalized scaling law for settlements of dry sand deposit. 15th World Conference on Earthquake Engineering, Portugal. 2012: No. 4104.

FIGURES AND TABLES

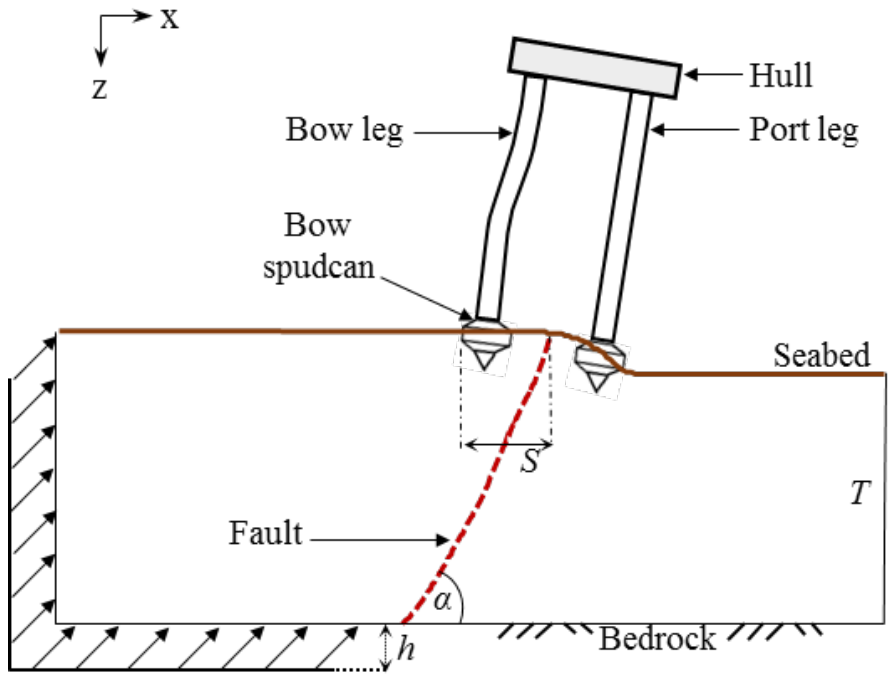

Figure 1**.** Schematic of the problem: reverse fault propagating and rupturing at the spudcan foundations. The initial dip of the fault at the bedrock-soil interface shown by α, fault throw, h and the thickness of the soil layer expressed as T. S denotes the distance from the left edge of the bow spudcan to the free-field fault rupture location.

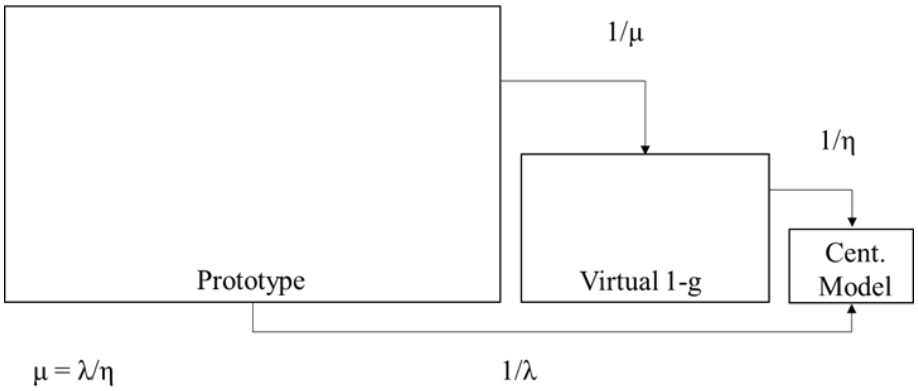

Figure 2. Relationship between the prototype, virtual 1 g model and the centrifuge model ($\lambda = \mu\eta$). Adapted from [19].

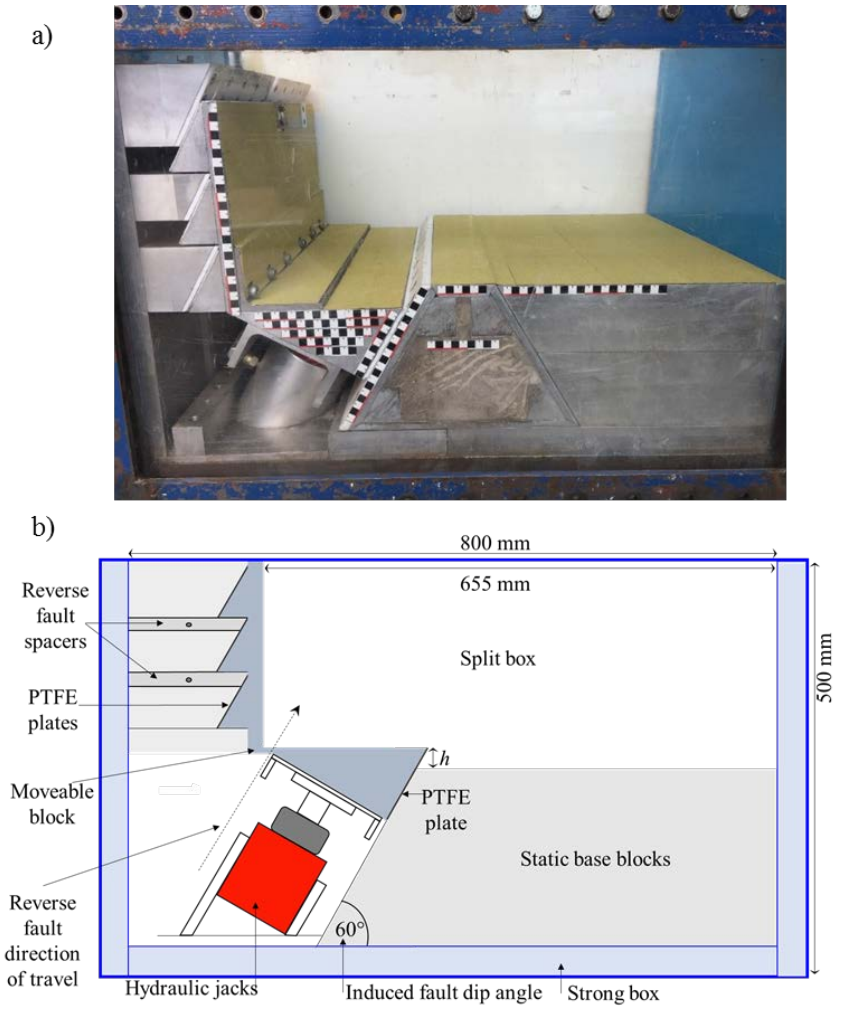

Figure 3. a) University of Dundee split box inside the centrifuge strong box and b) Simplified diagram of the split box contained within the centrifuge strong box. Induced faulting creates a fault throw *h* and a 60° dip angle.

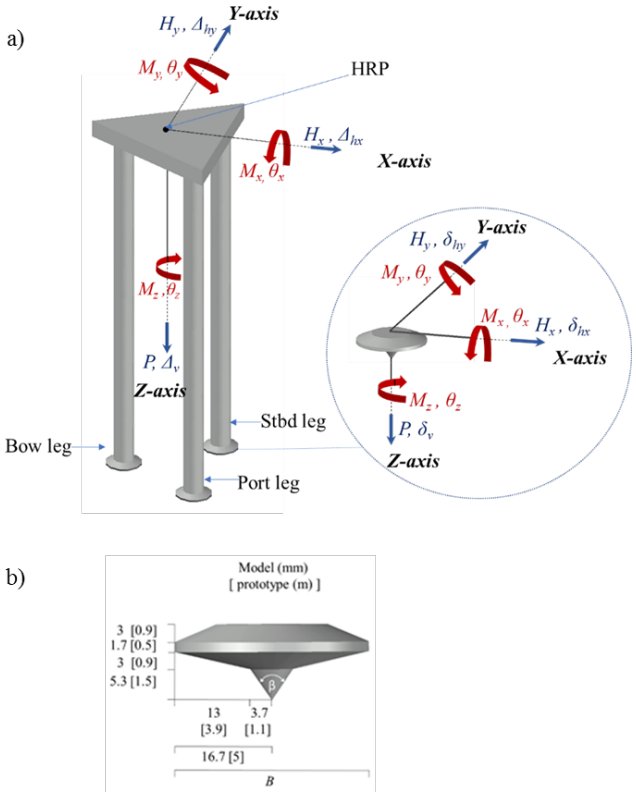

Figure 4. a) Sign conventions and loading directions. HRP is the hull reference point, bow is the front of the rig and stern the back and b) Spudcan dimensions, β denotes cone apex angle and *B* is the spudcan diameter.

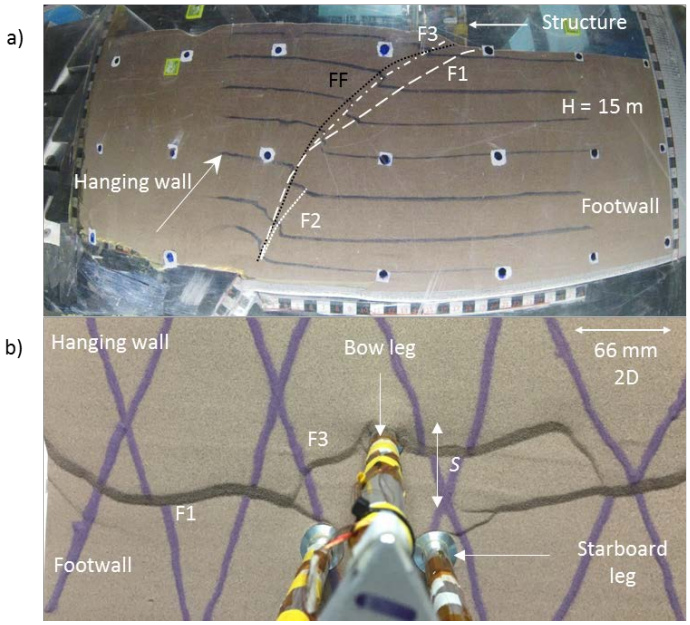

Figure 5. Reverse fault propagation and rupture at surface a) shows elevation profile of fault propagating through the soil. Hanging wall block is shifted upwards and to the right; b) shows a plan view from above the jack-up hull shows fault diversion around the footings of the structure. F1 is the primary fault. F2 and F3 show the expression of fault bifurcations. FF shows the propagation path of the fault in the free-field.

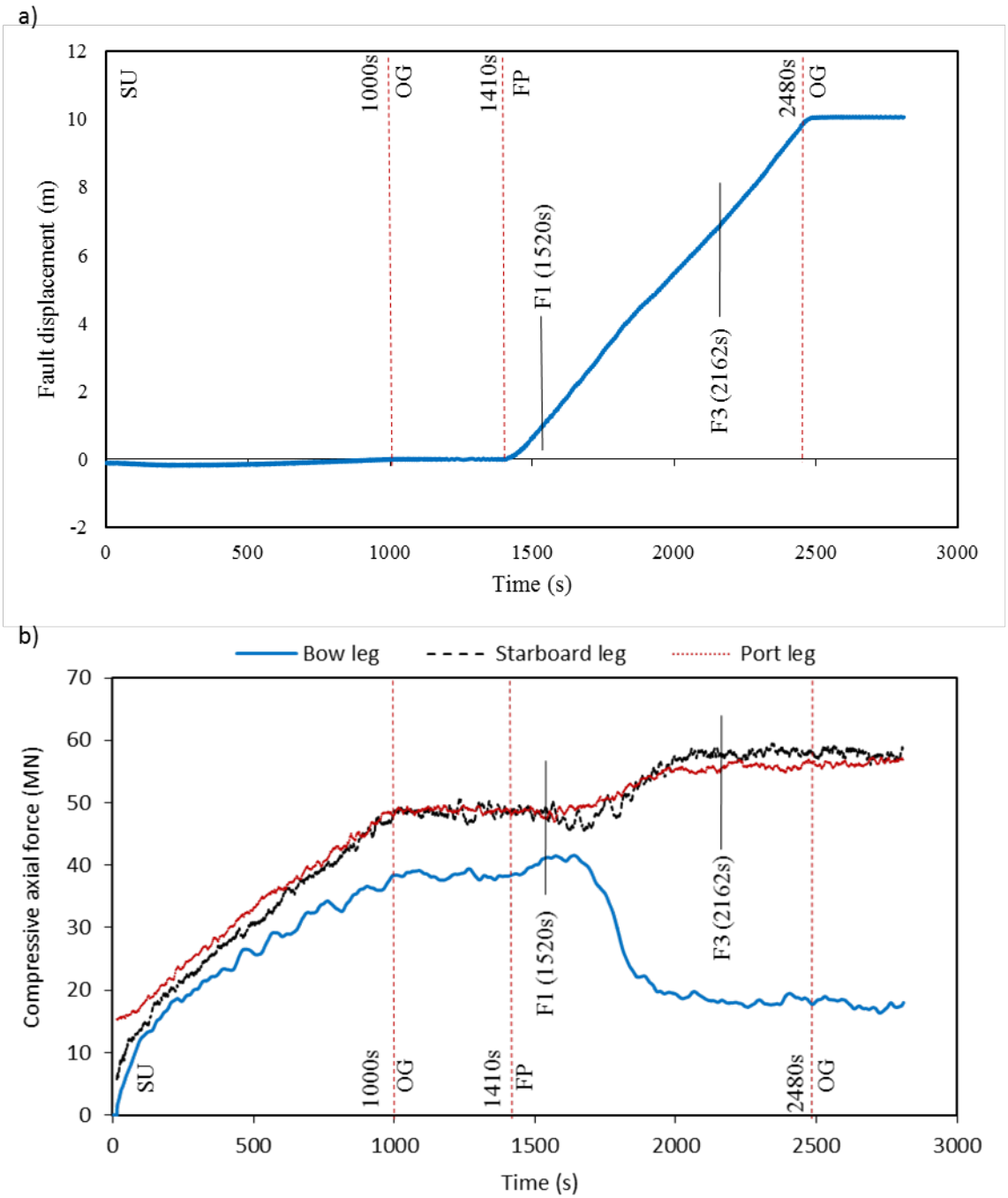

Figure 6. a) Prototype scale vertical fault displacement with test time, with the phases of the test represented by: SU = spin-up, OG = operating g-level, FP = faulting phase and F1 = F1 surface rupture (occurring at 1520 seconds), F3 = F3 surface rupture (occurring at 2162 seconds); b) Prototype scale compressive axial force with test time.

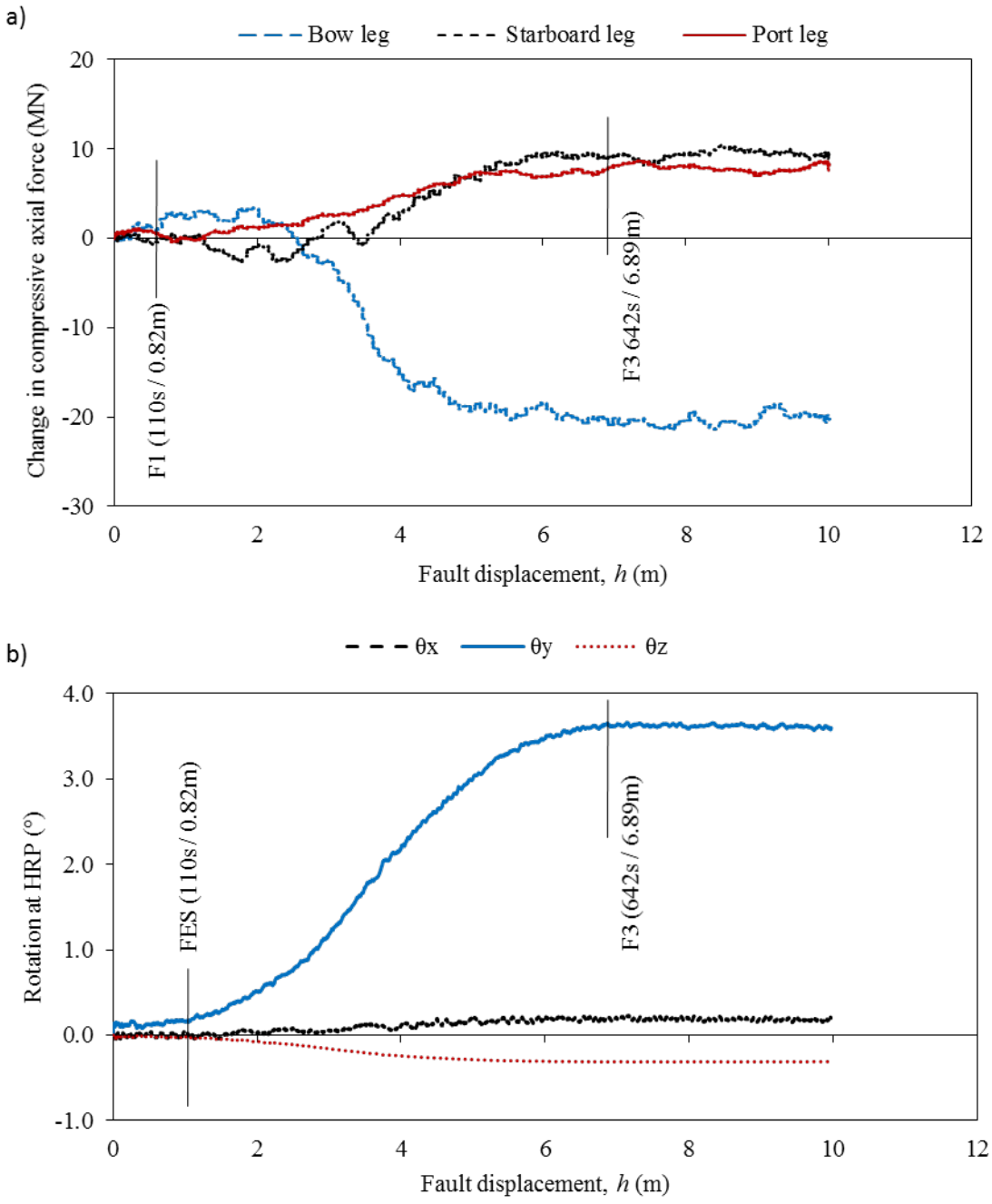

Figure 7. a) Prototype scale change in compressive axial force on spudcans with fault displacement, F1 = F1 surface rupture (occurring at 110 seconds into the faulting phase / 0.82m of displacement), F3 = F3 surface rupture (occurring at 642 seconds into the faulting phase / 6.89 m of displacement); b) Rotations at the hull reference point (HRP) with fault displacement.

Table 1. Key components of the jack-up structure

Structural components	**Model**	**Prototype**
Hull length x width x depth	83 x 90 x 20 (mm)	25 x 27 x 6 (m)
Spudcan diameter	33 (mm)	10 (m)
Leg length	296.67 (mm)	89 (m)
Lightship	0.5763 kg	15,560.37 t
Hull mass	0.3532 kg	8,494.39 t
One leg mass	0.0575 kg	1,553.04 t
One spudcan mass	0.0168 kg	454.68 t
EA_{leg}	14.3×10^6 (N)	5.7×10^8 (kN)
EI_{leg}	8.8×10^8 (N·mm^2)	1.4×10^9 (kN·mm^2)